Plasmon resonant (e, 2e) spectroscopy on Be(0001)

Gianluca Di Filippo,[1,*] Damiano Sbaraglia,[2] Alessandro Ruocco,[2] and Giovanni Stefani[2]
[1]*Scuola dottorale in Matematica e Fisica, Università degli Studi Roma Tre, via della Vasca Navale 84, I-00146 Rome, Italy*
[2]*Dipartimento di Scienze e Unità CNISM, Università degli Studi Roma Tre, via della Vasca Navale 84, I-00146 Rome, Italy*
(Received 2 August 2016; published 13 October 2016)

We investigated the mechanisms of secondary electron (SE) emission from Be(0001) by impact of 100 and 150 eV electrons. We made use of (e, 2e) spectroscopy to disentangle the different SE production mechanisms. We observed a large increase in the SE yield when the energy loss of the primary electron equals the characteristic energy of volume and surface plasmons. The line shape of the SE spectrum associated with plasmon excitation reveals that one relevant emission mechanism corresponds to direct single-particle excitation in which the plasmon energy and momentum are transferred to a valence band electron of the solid. The contributions to the SE yield associated with surface and volume plasmon excitation are comparable in the case of specular geometry, where the projectile momentum is mainly transferred perpendicular to the surface. On the contrary, the emission of SEs associated with surface plasmon excitation is significantly enhanced when the exchanged momentum lies close to the surface plane and electrons are emitted from Be surface state. This reflects the increased sensitivity to surface modes of the latter geometry. Finally, the coupling between the direct ionization channel and the plasmon-assisted one results in a resonant increase of the secondary emission.

DOI: 10.1103/PhysRevB.94.155422

I. INTRODUCTION

The inelastic scattering of electrons from solid surfaces has been one of the most important methods to study the electronic properties of materials. In the framework of the dielectric theory [1] the spectral response of a solid to an inelastic electron collision is determined by its bulk- and surface-loss function.

Prominent maxima in these functions correspond to the frequencies of collective excitation, so that one of the most efficient channels of electron impact energy transfer is the excitation of volume or surface plasmons.

In addition, the scattering process may also result in the ejection of low energy electrons that fall in the energy range usually covered by secondary electrons (SEs). Electron-induced SE emission is the most relevant result of the energy transfer mechanism and it is of fundamental interest in a broad variety of applications. It is currently employed in scanning electron microscopy [2] in which the investigated object is scanned by a focused electron beam while SEs are detected. The intensity of emitted electrons as a function of the beam position furnishes a detailed image of the sample surface. Furthermore, SE emission from surfaces as a result of energetic electron bombardment is a key process in the electrical charges of spacecrafts [3]. Its role is so important that the SE yield is a fundamental parameter in NASA spacecraft charging analysis programs [4]. In addition, SE generation limits the resolution and contrast in electron beam lithography, leading to an effective broadening of the beam diameter [5].

Despite its importance in many fields of applied physics, the origin of SEs is still questioned. In the past years, Chung and Everhart [6] first, and Bocan and Miraglia [7] later postulated plasmon decay to be the largest SE generation process. In their picture a plasmon excited by a scattered electron decays by transferring its energy and momentum to a valence band electron which is then emitted in the secondary region. Other mechanisms, e.g., plasmon decay by the emission of a pair of interacting electrons or direct electron-electron scattering, were considered negligible. In recent years, Kouzakov and Berakdar [8] proposed the ejection of a SE due to direct electron-electron scattering within a medium described by its inverse dielectric function. The screened Coulomb potential mediating the process is such that the scattering probability is resonant at energy transfers corresponding to the excitation of collective modes, such as volume or surface plasmons. The model predicts the general features [8] of the cross section measured on Al [9], but lacking the solid band structure it fails to describe fine details of it [10].

The experimental investigation of the SEs origin represents a difficult task due to a lack of clearly resolvable experimental features in SE spectra that does not allow us to experimentally separate the different production mechanisms. This is indeed a crucial problem, but it can be dealt with by means of (e, 2e) spectroscopy. The (e, 2e) process consists of detecting, coincident in time, the scattered and ejected electrons created by an incident electron beam [11–13]. If backscattered electrons are measured together with SEs, the (e, 2e) spectrum can furnish information on the mechanisms of SE production [9,14,15]. The band structure of the sample under investigation plays a fundamental role in the mechanism of the decay of plasmons. Recently it has been pointed out that the emitted electron after plasmon decay, in the case of Al, comes from the top of the conduction band or even from the surface state [9,10].

In this paper we investigated the mechanisms of SE emission from Be(0001) by means of (e, 2e) spectroscopy. The coincidence cross section revealed that a relevant channel of SE production corresponds to single-particle emission in which the full energy and momentum transferred to the plasmon are absorbed by one electron in the valence band. This results in a resonant increase in the SE yield when the energy loss suffered

*Present address: Lehrstuhl für Festkörperphysik, Friedrich-Alexander-Universität Erlangen-Nürnberg, Staudtstraße 7, 91058 Erlangen, Germany; gianluca.filippo@fau.de

by the scattered electron equals the energy of bulk (BP) and surface (SP) plasmon. The initial state of the emitted electrons can be reconstructed by applying energy and momentum conservation rules. We observed that the SE yield associated with plasmon excitation is intimately related to the sample band structure. Indeed electron emission is not observed if no occupied state is available for the plasmon-assisted scattering process.

As the experiment was performed on a single crystal, it has been possible to exploit a large variety of different kinematics in which the Bragg diffracted beams played the role of monochromatic incident beam for the inelastic collisions [16]. It implies further degrees of freedom in selecting both momentum transfer in the inelastic collision and momentum of the ejected electron. We observed that the relative contribution of BP and SP excitation to the SE yield varies with the scattering geometry. It essentially depends on the direction of the momentum transfer $\mathbf{K}$ in the inelastic scattering of the primary electron. We observed an increase of more than one order of magnitude in the SP contribution when the geometry is varied from normal ($\mathbf{K}_{\parallel} \ll \mathbf{K}_{\perp}$) to grazing ($\mathbf{K}_{\parallel} \gg \mathbf{K}_{\perp}$) scattering and SE are emitted from Be surface state. Here $\mathbf{K}_{\parallel}$ ($\mathbf{K}_{\perp}$) indicates the component of the momentum transfer parallel (perpendicular) to the surface. In the latter case the (e, 2e) signal essentially describes the emission of SEs from beryllium surface state.

II. EXPERIMENTAL ASPECTS

The experimental setup is schematically illustrated in Fig. 1. An electron gun is used to irradiate the sample with a monochromatic beam of energy E_0. Two hemispherical analyzers are used to record the energy-loss spectrum (analyzer 1) and SE spectrum (analyzer 2), with an accepted polar angle of $\pm 0.5^\circ$ and $\pm 2.0^\circ$, respectively. Coincidences are detected by means of a standard coincidence circuit described in detail elsewhere [9,10]. The coincidence intensity presents two contributions referred as "true" and "random" events. Random events are associated with the detection of two uncorrelated electrons which are accidentally coincident in time while true events correspond to the detection of two correlated electrons. In order to remove the aggregate effect of the random coincidences we followed standard procedures documented in the literature [17,18].

The main components of the experimental apparatus are flanged to a ultrahigh-vacuum chamber with a base pressure of 3×10^{-10} mbar. The whole apparatus is located within a large Helmholtz cage which compensates the Earth's magnetic field. A Be(0001) sample was mounted in the sample holder placed on a manipulator that allows the rotation around the polar direction θ and to vary the geometry of the experiment. This is defined by the angle that the incident and scattered electrons form with the normal to the sample surface, θ_i and θ_o, respectively. The mutual angle between the two analyzers is fixed and equal to 90°, so that the emission angle of the secondary electrons with respect to the sample surface equals θ_o. Three different geometries were adopted in order to investigate different scattering kinematics. They are displayed in Fig. 1 and will be described later in the text. The Be(0001) sample was cleaned by repeated cycles of

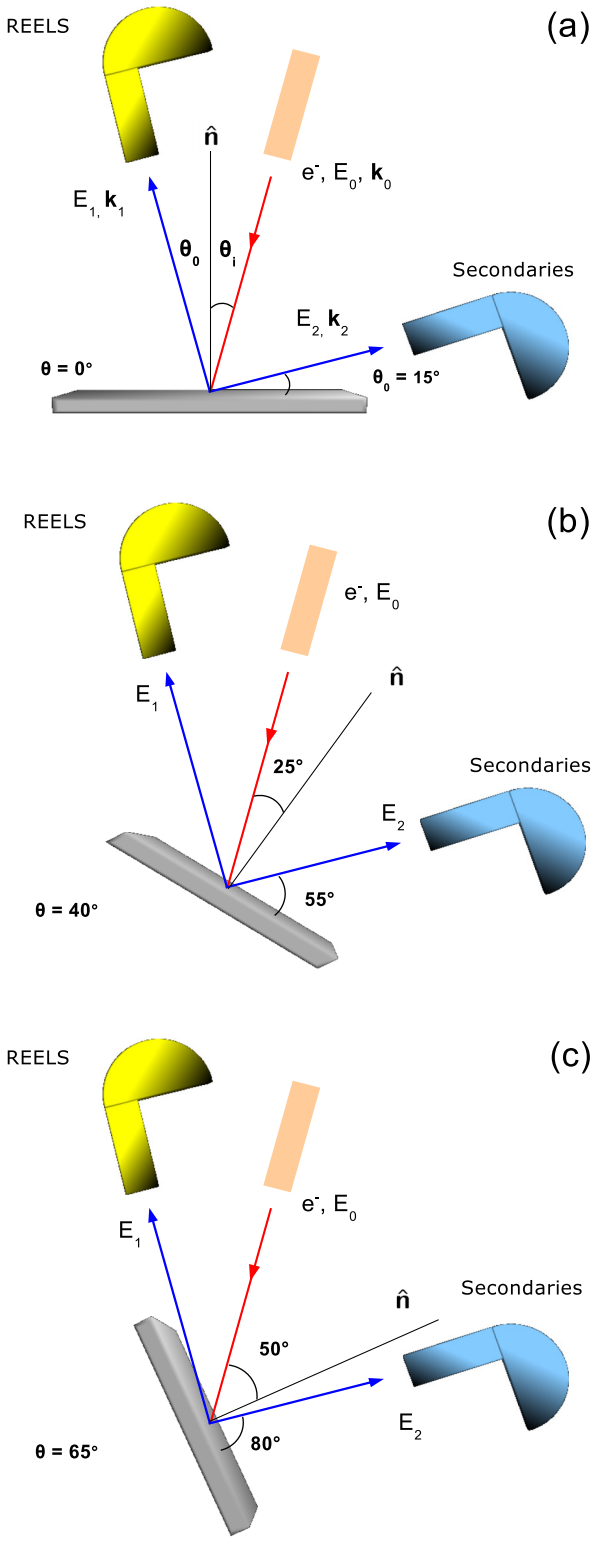

FIG. 1. Schematic of the experimental apparatus used to detect the reflected and secondary electrons in coincidence. The incoming beam of primary electrons strikes the sample with an incident angle θ_i, the reflected (energy-loss) electrons, emitted at an angle θ_o, are detected by the analyzer 1, while the secondaries are detected by the analyzer 2. The geometry of the experiment can be varied by rotating the sample around the polar angle θ. Three different geometries were adopted in the experiment: (a) $\theta_i = \theta_o = 15^\circ$ (specular reflection), (b) $\theta_i = 25^\circ$ and $\theta_o = 55^\circ$, and (c) $\theta_i = 50^\circ$ and $\theta_o = 80^\circ$.

2 keV Ar^+-ion sputtering and subsequent annealing at 450 °C. After the cleaning procedure the sample presented a good quality, sixfold LEED pattern with an oxygen contamination, whose estimation was obtained comparing the intensities of Be-1*s* and O-1*s* photoemission lines [19], well below 3% of the monolayer coverage. The LEED pattern was used to orient the scattering plane, i.e., the plane defined by the wave vector of the incident ($\mathbf{k}_0$) and scattered ($\mathbf{k}_1$) electron, along specific high-symmetry directions of the sample surface. The cleaning procedure was repeated (every 4–6 h) before starting a new coincidence measurement. The current of the primary beam was measured at each measurement by means of a Faraday cup mounted on the manipulator. Typical incident currents were of the order of 30 pA, corresponding to true-to-random ratio in the time spectra of about 0.5. Spectra were acquired in two different modes. (i) The SE spectrum was scanned ($3 \leqslant E_2 \leqslant 16$ eV) in coincidence with the energy-loss features associated with surface and bulk plasmon excitations, respectively. (ii) The energies of reflected and secondary electrons were scanned while the energy balance was maintained constant by fixing the sum energy $E_1 + E_2$ of the detected particles. We measured nearly 20 points for any of the presented coincidence spectra. Each point was measured for an average acquisition time of 5 h. Thus, the total accumulation time for each spectrum was $\sim$ 100 h leading to a statistical uncertainty around 10%. In order to check for the reproducibility of the experiment some of the points were measured more than once. In those cases the average value of all the measurements is reported.

III. EXPERIMENTAL RESULTS AND DISCUSSION

A. Momentum transfer close to normal

In Fig. 2 the SE spectrum measured by analyzer 2 alone (solid, green line) is compared to the SE spectrum in coincidence with the bulk plasmon loss (data points with error bars). For these two measurements, the analyzer detecting the scattered electrons was set to the characteristic energy loss of the bulk plasmon ($E_0 - E_1 = \hbar\omega_b = 18.4$ eV), while the other analyzer was scanned through the secondary spectrum. The energy of the incident electron beam was $E_0 = 100.6$ eV. Two different geometries were investigated. In the first one, displayed in Fig. 1(a), the coincidence spectrum (filled circles) was acquired in specular-reflection geometry, with $\theta_i = \theta_o = 15°$. In the second geometry (open diamonds) the sample was tilted to $\theta = 40°$ to obtain $\theta_i = 25°$ and $\theta_o = 55°$. This geometry, shown in Fig. 1(b), satisfies the Bragg condition for second order surface diffraction $\Delta\mathbf{k}_\parallel = \mathbf{k}_{0\parallel} - \mathbf{k}'_{0\parallel} = 2 \times \mathbf{g}_\parallel^{(\overline{\Gamma}\text{-}\overline{M})}$. Here $\mathbf{k}'_0$ is the wave vector of an elastically scattered electron and $\mathbf{g}_\parallel^{(\overline{\Gamma}\text{-}\overline{M})}$ is a primitive reciprocal lattice vector along the $\overline{\Gamma}$-$\overline{M}$ symmetry direction.

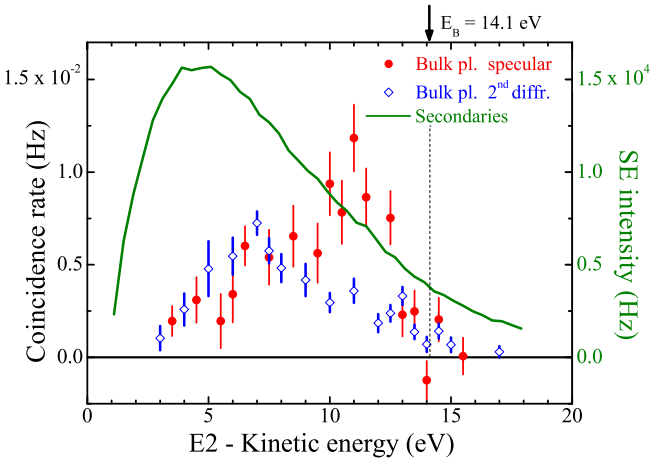

FIG. 2. Data points with error bars: The SE spectrum measured in coincidence with the bulk plasmon loss feature in the REELS spectrum. Filled circles are obtained in specular geometry. Open diamonds correspond to $\theta_i = 25°$ and $\theta_o = 55°$. The solid (green) curve represents the SE spectrum measured by analyzer 2 alone.

The coincidence spectra differ consistently from the SE spectrum for two reasons. First, plasmons contribute only partly to the SE yield. When high energy electrons travel into a solid, they can suffer multiple energy losses and give rise to a cascade of secondary electrons that is responsible for the rather featureless spectrum represented by the solid line in Fig. 2. Second, the plasmon contribution to the single SE spectrum results from the integration of the corresponding cross section over all the possible values of energy and momentum transfer. As we will shortly show, the coincident detection of two electrons consistently restricts the number of these values so that coincidence spectra always differ from the corresponding SE distribution.

The determination of the relative contribution of cascade and plasmon-assisted processes is of crucial interest. It will require the measurement of the absolute value of the corresponding cross sections which is beyond the scope of this work.

The intensity of the coincidence signal in specular geometry (filled circles) increases with the SE kinetic energy to its maximum value of $\sim 10^{-2}$ Hz in the region $10 \leqslant E_2 \leqslant 13$ eV. At higher kinetic energies a steep descent is observable, and the intensity vanishes above 15 eV. The dashed vertical line in Fig. 2 is located at a threshold energy $E_B = 14.1$ eV, corresponding to the energy loss of the bulk plasmon minus the analyzer work function ($\phi_A = 4.3$ eV). This corresponds to the kinetic energy of electrons emitted from the Fermi level, if all the energy loss and momentum transfer of the incident electron are transferred to a valence band electron. The coincident SE line shape in diffraction geometry (open diamonds) shows an ascending trend at low-kinetic energy, and reaches its maximum ($\sim 0.5 \times 10^{-2}$ Hz) for $E_2 = 7$ eV. Then the coincidence yield decreases monotonically and vanishes above the threshold energy.

The measured spectra show significant differences, especially in the energy region $E_2 \geqslant 10$ eV. These can be understood if one considers that the coincidence line shapes are determined by the energy of the plasmon losses, the momentum transfer $\mathbf{K}$, and the band structure of beryllium. Taking this into account it can be shown that the differences between the specular and diffraction geometry data reflect changes in the initial states of the electrons involved in the emission process. The initial binding energy E_b and momentum $\mathbf{q}$ of the valence band electrons inside the solid

are given by the conservation laws [21]:

$$E_b + \phi_A = E_0 - E_1 - E_2, \tag{1}$$

$$\mathbf{q}_\parallel = \mathbf{k}_{1\parallel} + \mathbf{k}_{2\parallel} - \mathbf{k'}_{0\parallel} + \mathbf{g}_\parallel, \tag{2}$$

where E_0 is the energy of the primary beam, $\mathbf{g}$ is a reciprocal lattice vector, and E_1 and E_2 ($\mathbf{k}_1$ and $\mathbf{k}_2$) are the kinetic energy (momentum) of the inelastically scattered and emitted electrons, respectively. According to former works [16], plasmon excitation observed in reflection geometry are dominated by two-step processes in which the inelastic collision is accompanied by an elastic one. In the considered geometries (aligned to the diffraction condition for the primary beam) the elastic event precedes the inelastic one [16]. This explains why the momentum of the elastically diffracted electron $\mathbf{k'}_0$ is contained in the equation. Under this assumption the momentum transfer in the inelastic scattering corresponds to $\mathbf{K} = \mathbf{k'}_0 - \mathbf{k}_1$. When the electrons pass through the surface potential barrier in their penetration or escape from the sample, their momenta components perpendicular to the surface are modified. Therefore, momentum conservation can be only applied to the parallel components of the measured and primary electrons to obtain the parallel momenta of the valence band electrons in their initial state. In the performed experiments, the energy difference between the incident and scattered electron equals the plasmon energy $E_0 - E_1 = \hbar\omega_p$. This allows us to rewrite relation (1) in a more direct way and to relate the kinetic energy of the detected SE to the binding energy of its initial bound state,

$$E_b = \hbar\omega_p - E_2 - \phi_A. \tag{3}$$

Figure 3 shows the projection of Be bulk bands and the surface state calculated by Chulkov *et al.* [20] along $\overline{\Gamma}$-$\overline{M}$ symmetry direction. The black dots within the rectangular boxes represent the regions of the $(\mathbf{q}_\parallel, E_b)$ space reconstructed in specular [Fig. 3(a)] and diffraction [Fig. 3(b)] geometry. The different geometries, depicted in the corresponding insets, lead to different cuts in the sample occupied (shaded regions) and unoccupied (white regions) states. The height and width of the sampled regions are dictated by energy and momentum resolution, respectively. The former is constant and equal to $\Delta E = 3.0$ eV. The latter, related to energy and angle resolutions, ranges from 0.2 to 0.4 Å^{-1}. The sampled regions are directly related to the corresponding coincidence spectra. In specular reflection, Fig. 3(a), for low-kinetic-energies ($E_2 \leqslant$ 6 eV) the reconstructed points correspond to an energy gap in the band structure. This means that no electron can be excited and this results in a low coincidence rate. When the kinetic energy of the SE increases the reconstructed regions in the momentum space starts to overlap the occupied states and this leads to an increase in the SE yield. The maximum superposition is reached for energies included between 10 and 12 eV, this corresponding to the zone of maximum intensity in the coincidence spectrum. A further increase in the SE kinetic energy is equivalent to excite electrons near the Fermi edge. The superposition between the sampled areas and the occupied states decreases when moving towards lower binding energies. This can be identified in the decrease of the coincidence rate around the threshold energy. These energies

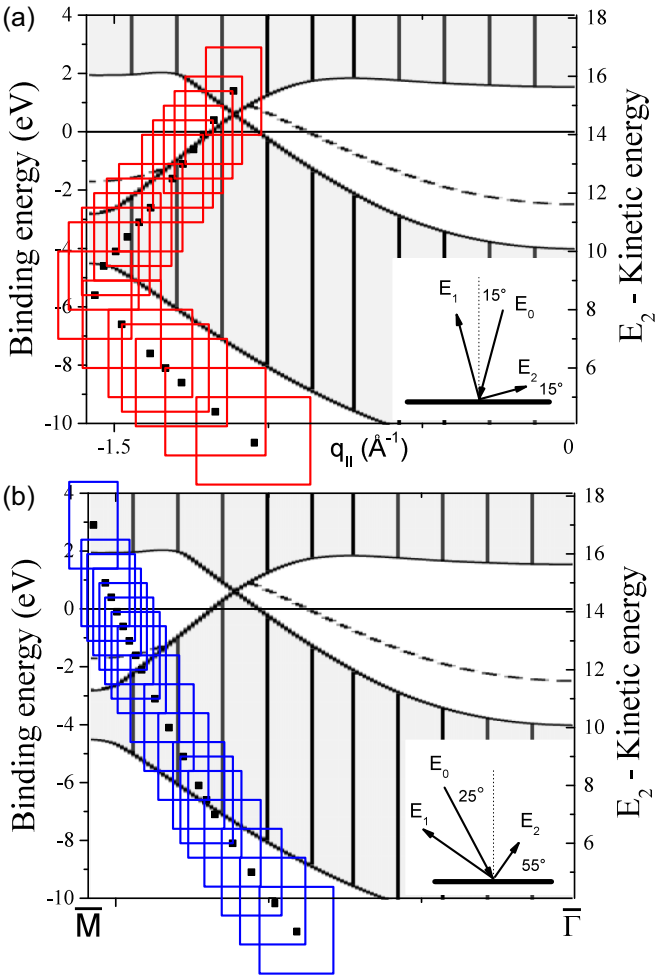

FIG. 3. Black dots: Initial momentum and binding energy of the SEs emitted in the volume plasmon decay for the geometry depicted in (a) Fig. 1(a) and (b) Fig. 1(b). The boxes represent the amplitude of the reconstructed regions due to energy and momentum resolution of the experimental setup. The background is adapted from Ref. [20] with permission of Elsevier. It represents the calculated Be(0001) band structure. The shaded region is the projection of Be bulk bands. The dashed line shows the dispersion of the surface state.

also correspond to the excitation of electrons from the surface level (dashed line in Fig. 3), but the surface state contribution cannot be distinguished from the bulk states one. This might be due to the poor energy resolution. When the SE energy exceeds the threshold value E_B, energy conservation results in (unoccupied) initial states above the Fermi level, and the SE yield drops to zero.

Analogous considerations can be drawn when tuning on losses generated by the Bragg diffracted beam, Fig. 3(b). In this case, the sampled areas in the $(\mathbf{q}_\parallel, E_b)$ space show optimal superposition with the occupied states for energies of the emitted electrons between 6 and 11 eV. This is directly reflected in the line shape of the spectrum acquired in Bragg diffraction geometry. Most of the spectral weight is centered in the above mentioned energy window, while a descent is observed in the high- and low-kinetic energy side. In analogy to the specular case, no emission is observed above threshold.

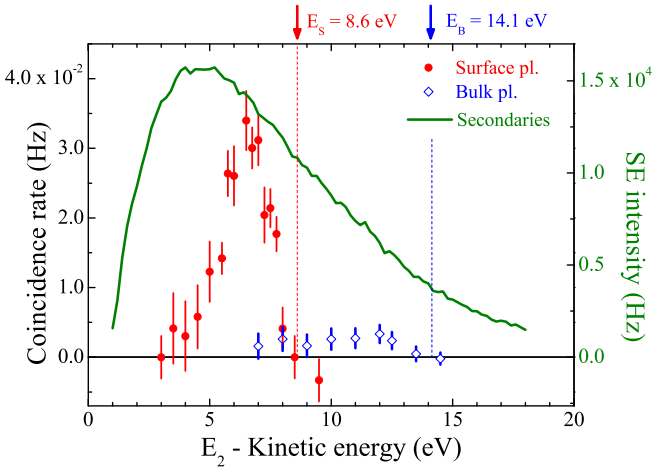

FIG. 4. Data points with error bars: The SE spectrum measured in coincidence with the surface (filled circles) and bulk (open diamonds) loss features in the REELS spectrum. The incidence and reflection angles are $\theta_i = 50^\circ$ and $\theta_o = 80^\circ$, respectively. The solid (green) curve represents the SE spectrum measured by analyzer 2 alone.

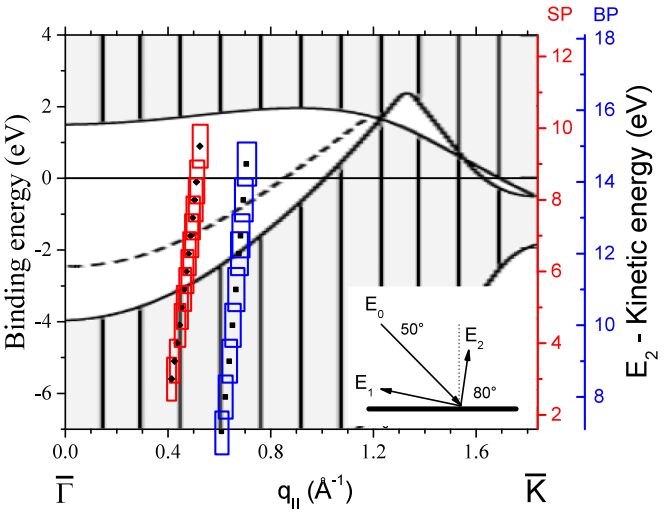

FIG. 5. Initial momentum and binding energy of the SE emitted in the surface (diamonds) and volume (squares) plasmon decay reconstructed using Eqs. (2) and (3). The boxes represent the amplitude of the reconstructed regions due to energy and momentum resolution of the experimental setup. The kinetic energy of the emitted secondary electrons is indicated in the right scale for surface (SP) and volume (BP) plasmon, respectively. The background is adapted from Ref. [20] with permission of Elsevier. It represents the calculated Be(0001) band structure. The shaded region is the projection of Be bulk bands. The dashed line shows the dispersion of the surface state.

The connection between the reconstructed regions and the coincidence spectra proves that in the plasmon-assisted (e, 2e) process electrons are emitted via the creation of a single electron-hole pair for single plasmon. Additional emission mechanisms, involving other particles such as another electron or a phonon, are less favorable. In these latter transitions, conservation rules in (1) and (2) must be modified to take into account the energy and momentum of the extra particle. Therefore, the correspondence between coincidence spectra and reconstructed regions in the momentum space is lost, and a continuous distribution (that is not observed) will be expected.

B. Grazing momentum transfer

Figure 4 shows the SE spectrum measured in coincidence with the energy-loss features connected to the surface (filled circles) and bulk (open diamonds) plasmon. The adopted geometry is displayed in Fig. 1(c). The primary electron beam of kinetic energy $E_0 = 150.6$ eV hit the sample with an incident angle $\theta_i = 50^\circ$. The reflected electrons ($E1 = 137.7$ and $E1 = 132.2$ eV for surface and bulk plasmon, respectively) were detected by analyzer 1 at an angle $\theta_o = 80^\circ$, while the SE spectrum was scanned by analyzer 2. This configuration was chosen in order to satisfy the Bragg condition for second order diffraction along Be(0001) $\overline{\Gamma}$-$\overline{K}$ direction, $\Delta\mathbf{k}_\parallel = 2 \times \mathbf{g}_\parallel^{(\overline{\Gamma}\text{-}\overline{K})}$. In order to resolve the contributions to the SE yield ascribable to the excitation of electrons located within the bulk or surface states, the energy and momentum resolution of the coincidence spectrometer were improved. This was achieved by reducing the pass energy of analyzer 1 (from 73 to 25 eV) and analyzer 2 (from 70 to 40 eV). With these settings energy and momentum resolutions of $\Delta E = 1.2$ eV and $0.03 \leqslant \Delta\mathbf{q}_\parallel \leqslant 0.07$ Å^{-1} were attained. The coincidence spectra are compared to the SE spectrum (measured by analyzer 2) represented by the solid line. The dashed lines at $E_S = 8.6$ eV and $E_B = 14.1$ eV define the maximum energy accessible to the SEs emitted in coincidence to surface (SP) and bulk plasmon (BP) excitation, respectively. The surface plasmon-secondary coincidence spectrum (circles) consists of a sharp and intense peak located ∼2 eV below the corresponding threshold energy. The peak is not symmetric and shows some extra emissions in its low-kinetic-energy side, $E_2 \leqslant 5$ eV. The bulk plasmon-secondary coincidence spectrum (diamonds) presents a nonzero coincidence rate up to a maximum kinetic energy $E_2 \sim 12$ eV. It shows an analogy with the surface plasmon one, with the falling edge of the distribution located 2 eV below the corresponding threshold. On the contrary, the coincidence intensity is not peaked at this energy but is continuously distributed over the SEs energy window.

In analogy to what has been done for the bulk plasmon one can reconstruct the initial binding energy and momentum of the emitted electrons. Figure 5 shows the regions of the $(\mathbf{q}_\parallel, E_b)$ space sampled in correspondence to surface (diamonds within the red boxes) and volume (squares within the blue boxes) plasmon excitation, respectively. The experimental conditions were chosen in such a way that the performed cuts overlap both the projection of the bulk states (shaded region) and the surface state (dashed line) of Be(0001) electronic structure. The BP coincidence spectrum shows nonvanishing intensity as long as portions of the occupied bulk states are sampled, $E_2 \leqslant 12$ eV. The leading edge of the distribution ($E_2 = 12$ eV) corresponds to the emission of electrons from the top of the valence band. Higher kinetic energies of the emitted electrons correspond to reconstructed regions located within the energy gap around the Fermi level. This is the reason why the coincidence intensity rapidly drops for $E_2 \geqslant 12$ eV. Here it is important to notice that no clear contribution from the surface state is observed.

The dispersion of this state is such that its binding energy (for the $\mathbf{q}_{\parallel}$ sampled in the BP experiment) is around 1 eV, see the dashed line in Fig. 5. According to energy conservation (3), the emission of electrons from the surface state should give rise to extra intensities at $E_2 = 13.1$ eV. The absence of such a structure suggests that the contribution to SE emission associated with bulk plasmon excitation is mainly ascribable to the emission of electrons from bulk states. This finding is at odds with a recent coincidence experiment on Al(100) [10]. Here the SE spectrum in coincidence with BP is dominated by emission from the Al surface state. We do not have a definitive explanation about the different results between Be and Al. A possible reason might reside in the different energy position of their respective surface states. Be(0001) surface state lies around 1.5 eV above the projected bulk band edge, i.e., around midgap. On the contrary, the surface state on Al(100) is only 0.1–0.3 eV above the bulk band [10,22,23]. The position of a surface state with respect to the projected bulk band has a strong influence on its properties [20,24]. In particular, it defines how deep it propagates into the bulk of the crystal. The closer it lies to the bulk levels, the deeper it penetrates into the solid. In the limiting case of a *surface resonance* the state is degenerate with the bulk bands and it propagates deep into the bulk but still retaining a large amplitude at the surface [1]. The lower penetration of Be(0001) surface state into the bulk and consequently the lower superposition with the corresponding bulk plasmon might be the reason behind the negligible coincidence yield associated with the emission of electrons from this state. This is only a speculative hypothesis. In order to have a deeper understanding of the observed phenomenon additional experimental and theoretical investigations are needed.

The above picture is reversed when the SE spectrum is measured in coincidence with the SP loss feature. In this case the coincidence spectrum corresponds to a sharp and intense peak located at $E_2 = 7$ eV. The energy balance for this coincidence event corresponds to the emission of electrons from the surface state located ∼2 eV below the Fermi level. Above this energy no electron is available for the emission and the coincidence intensity rapidly decreases and vanishes for energies above the threshold value of $E_2 = 8.6$ eV. The extra intensities observed in the low-kinetic-energy side of the main peak correspond to the emission of electrons from the bulk states. Indeed, for kinetic energies below 6 eV the sampled regions in the momentum space consistently overlap the occupied bulk states of the sample.

In this experiment the intensity of the SE yield is one order of magnitude higher in the case of the SP excitation than in the BP one. Thus, in the considered geometry most of the SEs are ejected from the surface state in correspondence to the excitation of a surface plasmon. For sake of completeness we also compared the intensities of bulk and surface plasmon coincidence signals in specular reflection geometry. In this case the surface signal corresponds to one third of the volume one. In a simplified picture the differences in surface and bulk plasmon-resonant scattering intensities can be understood in terms of the increased sensitivity to surface plasmon modes when passing from specular scattering to second order diffraction. In an inelastic-scattering experiment one sees only those modes whose electronic dipole moment

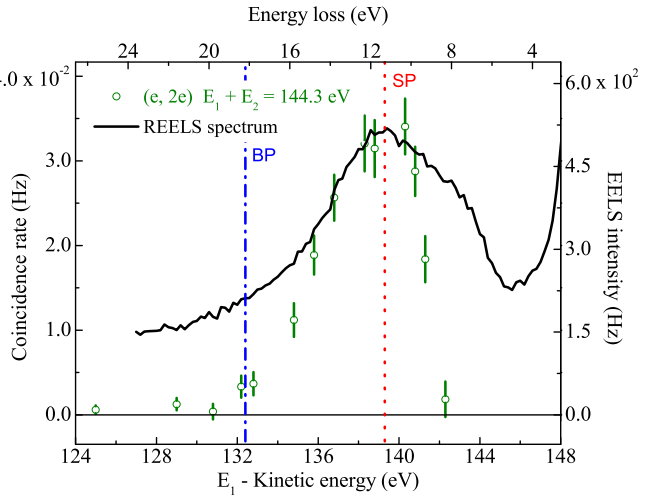

FIG. 6. Circles with error bars: SE spectrum measured in coincidence with the REELS spectrum for $E_1 + E_2 = 144.3$ eV. Solid line: Single REELS spectrum measured by analyzer 1. The dotted and dash-dotted lines represent the measured energies of the surface (SP) and bulk (BP) plasmon loss features, respectively.

is in the direction of the momentum transfer $\mathbf{K}$ [1]. This means that in specular scattering modes perpendicular to the surface are mainly observed. The opposite is for scattering direction close to the surface plane. Here the component of $\mathbf{K}$ parallel to the surface ($\mathbf{K}_{\parallel} = 0.27$ Å^{-1}) dominates over the normal one ($\mathbf{K}_{\perp} = 0.05$ Å^{-1}). Surface plasmons correspond to longitudinal magnetic modes propagating parallel to the vacuum/metal interface [25]. The corresponding electric field is such that electronic displacement, i.e., electric dipole moment, is mainly in the propagation direction [26,27]. This results in a very high probability to excite a surface plasmon when the momentum transfer is close to the surface plane. This can be clearly observed in the energy loss spectrum of Fig. 6 (thick line). Here the intensity of the surface plasmon loss at $E_1 = 139.2$ eV dominates the spectrum, whereas the bulk plasmon one, indicated by the dash-dotted line at $E_1 = 132.2$ eV, is almost indiscernible from the background.

All the presented results point to the fact that the electronic structure of the investigated system plays a fundamental role in determining the line shape of plasmon-assisted scattering spectra. The process can be schematically depicted as a photoemission event in which the plasmon plays the role of the photon. Applying energy and momentum conservation allows us to determine the initial state of the emitted electrons and ultimately to reconstruct the occupied portion of the band structure. Distinct scattering geometries can be more or less surface sensitive so that both bulk and surface states are accessible.

C. Direct and resonant ionization

The previous measurements cannot completely enlighten the contribution of plasmon excitation to SE production. As a matter of fact the acquired coincidence spectra might also be described in terms of direct electron-electron scattering. In this process the incoming electron directly interacts with a valence band electron. As a result of the interaction a part of the projectile energy and momentum are transferred to

the bound electron which is emitted in the SEs region. The whole process does not require the presence of any plasmon. In order to enlighten the role of plasmon-assisted scattering to the SE yield a complementary measurement is needed. The ideal would be to measure a spectrum at fixed initial state and to observe how the coincidence intensity varies with the energy loss $\Delta E = E_0 - E_1$. If plasmon-assisted scattering takes place we are in the presence of two alternative channels leading to the same final state. The coupling between them would result in a resonant increase in the (e, 2e) signal at energy losses corresponding to plasmon excitation. Unfortunately, the kinematic of the experiment does not allow us to simultaneously fix the binding energy and wave vector of the initial state. This is because the momenta of scattered and emitted electron, $\mathbf{k}_1$ and $\mathbf{k}_2$, vary with the corresponding kinetic energy. The condition closer to a fixed initial state corresponds to record a constant binding energy spectrum. According to (1) this condition is fulfilled if the sum energy $E_1 + E_2$ of the detected particles is kept constant. Figure 6 compares the energy loss spectrum (solid, black line) measured at $E_0 = 150.6$ eV and $\theta_i = 50^\circ$ with the (e, 2e) spectrum corresponding to $E_1 + E_2 = 144.3$ eV (circles, green). The selected energy balance was chosen in order to study the emission of electrons located ~2.1 eV below the Fermi edge, i.e., the nominal binding energy of the surface state. The vertical lines indicated with BP and SP correspond to the measured kinetic energy of bulk and surface plasmon, respectively. Once again, by means of Eqs. (2) and (3) we were able to reconstruct the initial energy and momentum of the ejected electrons. They are reported as the black dots inside the rectangular boxes (accounting for energy and momentum resolution) in Fig. 7 and compared to the surface band structure of the sample. The kinetic energy of the scattered electron increases from the right to the left of the figure, as indicated by the arrow on the top axis. The vertical lines correspond to the reconstructed $\mathbf{q}_\parallel$ when the energy loss of the scattered electron equals the surface (red, dotted line) and bulk (blue, dash-dotted line) plasmon energy.

The constant-sum-energy spectrum in Fig. 6 characterizes the dependence of the SE yield on the energy loss (top axis) of the primary electron. It starts to grow at $\Delta E =$ 8 eV and rapidly increases exhibiting maximum ($\sim 3 \times 10^{-2}$ Hz) at $\Delta E = 11.8$ eV. This corresponds to the energy of the surface plasmon excitation $\hbar\omega_s$ in the considered scattering geometry. Then it rapidly decreases down to negligible values at $\Delta E \geqslant 19.5$ eV. The contribution of the volume plasmon gives probably rise to the weak shoulder at $\Delta E = \hbar\omega_b \sim$ 18 eV.

The recorded (e, 2e) spectrum allows us to determine the contribution of plasmon excitation to the SE yield. For energy losses well above $\hbar\omega_s$ and $\hbar\omega_b$ the coincidence signal is proportional to the direct ionization cross section. The initial state of the emitted electron does not change significantly with the energy loss. Thus we do not expect that the direct scattering intensity ($\sim 0.5 \times 10^{-3}$ Hz) varies significantly in the whole spectrum. The increase of the coincidence intensity when the energy loss corresponds to the excitation energies of bulk and surface plasmon is striking evidence that the spectra we presented in the previous section essentially depict the plasmon-resonant scattering cross section.

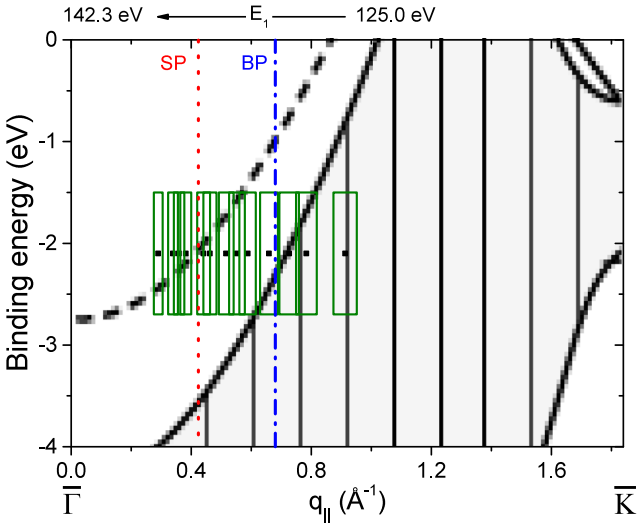

FIG. 7. Initial momentum and binding energy of the SE emitted in the constant sum energy (e, 2e) experiment. The boxes represent the amplitude of the reconstructed regions due to energy and momentum resolution of the experimental setup. The kinetic energy of the scattered (emitted) electron increases (decreases) from right to left. The dotted lines represents the reconstructed momentum for energy losses equal to the surface (SP) and volume (BP) plasmon energy. The background is adapted from Ref. [20] with permission of Elsevier. It represents the calculated Be(0001) band structure.

IV. SUMMARY AND CONCLUSIONS

In summary, we experimentally investigated the electron-energy-loss process followed by the emission of one secondary electron from Be(0001) surface. We made use of (e, 2e) spectroscopy to correlate the electron giving rise to the surface or bulk excitation with the corresponding SE. By measuring the SE spectrum in coincidence with volume and surface plasmon losses we observed that the main electron ejection mechanism corresponds to the one in which the energy loss ΔE and momentum transfer $\mathbf{K}$ needed to excite a plasmon are entirely transferred to a single valence band electron. The scattering vector $\mathbf{K}$ plays an important role in determining the relative contribution of SP and BP to the emission of secondary electrons. The emission correlated to SP excitation is resonantly increased when $\mathbf{K}$ is moved from near-normal ($\mathbf{K}_\parallel \ll \mathbf{K}_\perp$) to grazing ($\mathbf{K}_\parallel \gg \mathbf{K}_\perp$) direction and electrons are emitted from Be surface state.

As stated in the Introduction two mechanisms are predicted to bring to the ejection of SEs in the presence of a plasmonic excitation: screened electron-electron scattering [8] and plasmon decay [6,7]. In our experiment it is not possible to discriminate between the two contributions so that we cannot say which one of the two mechanisms prevails in beryllium. To this end, the comparison between the presented results and theoretical predictions taking into account the two mechanisms and the full band structure of the system would bring further information about the mechanism of SEs production.

Independently from the production mechanisms our experiment shows a resonant increase of SE emission in

coincidence with the excitation of one collective mode of the metal. These results emphasize the possibility to build up an energy- and momentum-resolved resonant spectroscopy, extremely suitable to investigate surface and interface states of metals.

ACKNOWLEDGMENTS

Partial financial support through SIMDALEE2 Sources, Interaction with Matter, Detection and Analysis of Low Energy Electrons 2 Marie Sklodowska Curie FP7-PEOPLE-2013-ITN Grant No. 606988 is greatly acknowledged.

[1] H. Lüth, *Solid Surfaces, Interfaces and Thin Films*, 4th ed. (Springer, Berlin, 2001), pp. 172–190.
[2] L. Reimer, *Scanning Electron Microscopy*, 2nd ed. (Springer, Berlin, 1998).
[3] I. Katz, M. Mandell, G. Jongeward, and M. S. Gussenhoven, J. Geophys. Res. [Space Phys.] **91**, 13739 (1986).
[4] M. J. Mandell, P. P. Stannard, and I. Katz, *NASCAP Programmer's Reference Manual* (National Aeronautics and Space Administration Lewis Research Center, Cleveland, OH, 1993).
[5] N. Samoto and R. Shimizu, J. Appl. Phys. **54**, 3855 (1983).
[6] M. S. Chung and T. E. Everhart, Phys. Rev. B **15**, 4699 (1977).
[7] G. A. Bocan and J. E. Miraglia, Phys. Rev. A **71**, 024901 (2005).
[8] K. A. Kouzakov and J. Berakdar, Phys. Rev. A **85**, 022901 (2012).
[9] W. S. M. Werner, A. Ruocco, F. Offi, S. Iacobucci, W. Smekal, H. Winter, and G. Stefani, Phys. Rev. B **78**, 233403 (2008).
[10] A. Ruocco, W. S. M. Werner, M. I. Trioni, S. Iacobucci, and G. Stefani (unpublished).
[11] J. Kirschner, O. M. Artamonov, and S. N. Samarin, Phys. Rev. Lett. **75**, 2424 (1995).
[12] F. O. Schumann, J. Kirschner, and J. Berakdar, Phys. Rev. Lett. **95**, 117601 (2005).
[13] A. Liscio, A. Ruocco, G. Stefani, and S. Iacobucci, Phys. Rev. B **77**, 085116 (2008).
[14] W. S. M. Werner, F. Salvat-Pujol, W. Smekal, R. Khalid, F. Aumayr, H. Störi, A. Ruocco, and G. Stefani, Appl. Phys. Lett. **99**, 184102 (2011).
[15] W. S. M. Werner, F. Salvat-Pujol, A. Bellissimo, R. Khalid, W. Smekal, M. Novák, A. Ruocco, and G. Stefani, Phys. Rev. B **88**, 201407 (2013).
[16] A. Ruocco, M. Milani, S. Nannarone, and G. Stefani, Phys. Rev. B **59**, 13359 (1999).
[17] G. Stefani, L. Avaldi, and R. Camilloni, in *New Directions in Research with Third-Generation Soft X-Ray Synchrotron Radiation Sources*, edited by A. S. Schlachter (Kluwer Academic, Amsterdam, 1994), pp. 161–188.
[18] E. Jensen, R. A. Bartynski, S. L. Hulbert, and E. D. Johnson, Rev. Sci. Instrum. **63**, 3013 (1992).
[19] C. S. Fadley, in *Electron Spectroscopy: Theory, Techniques and Applications*, edited by C. R. Brundle and A. D. Baker (Pergamon, Oxford, 1978), Chap. 3, p. 73.
[20] E. Chulkov, V. Silkin, and E. Shirykalov, Surf. Sci. **188**, 287 (1987).
[21] O. Artamonov, S. Samarin, and J. Kirschner, Appl. Phys. A **65**, 535 (1997).
[22] H. J. Levinson, F. Greuter, and E. W. Plummer, Phys. Rev. B **27**, 727 (1983).
[23] J. Inglesfield and G. Benesh, Surf. Sci. **200**, 135 (1988).
[24] R. A. Bartynski, E. Jensen, T. Gustafsson, and E. W. Plummer, Phys. Rev. B **32**, 1921 (1985).
[25] S. A. Maier, *Plasmonics: Fundamentals and Applications* (Springer, New York, 2007).
[26] W. L. Barnes, A. Dereux, and T. W. Ebbesen, Nature (London) **424**, 824 (2003).
[27] T. W. Ebbesen, C. Genet, and S. I. Bozhevolnyi, Phys. Today **61**, 44 (2008).